

# Lawrence Berkeley National Laboratory

## LBL Publications

### Title

Search for Nonminimal Neutral Bosons from Z-Boson Decays

### Permalink

<https://escholarship.org/uc/item/3ns791xn>

### Authors

Komamiya, S.  
Abrams, G.S.  
Adolphsen, C.E.  
et al.

### Publication Date

1990-06-11



# Lawrence Berkeley Laboratory

UNIVERSITY OF CALIFORNIA

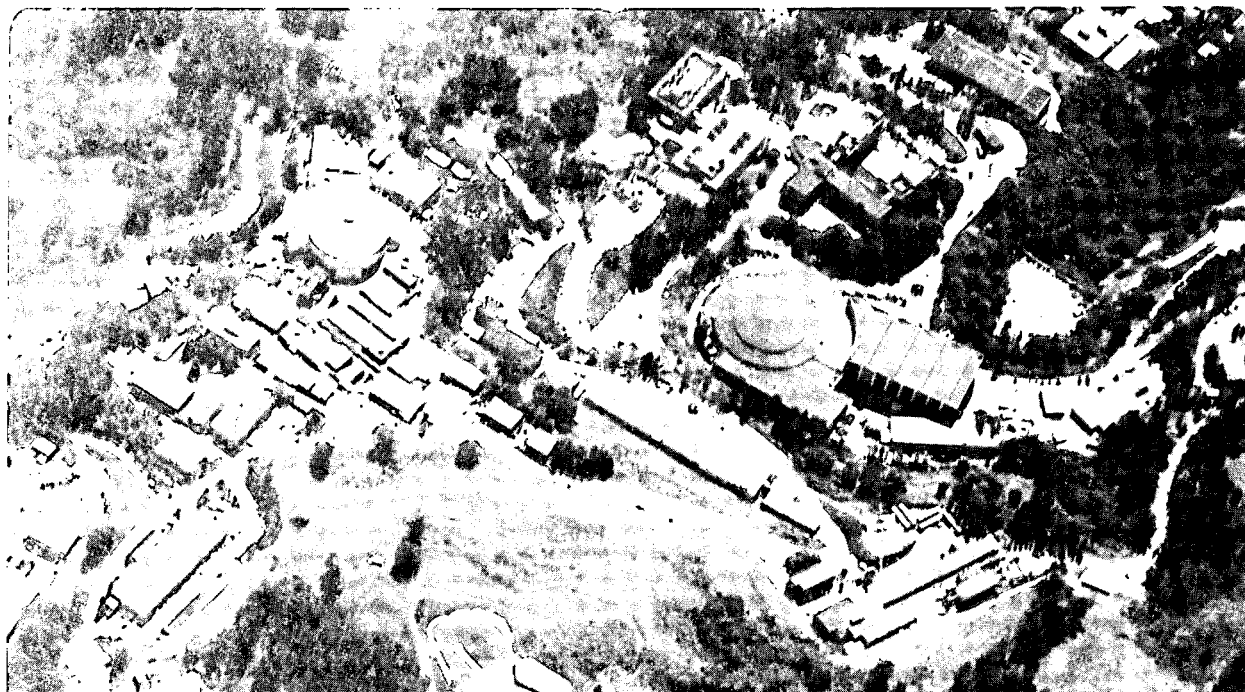
## Physics Division

Presented at the 1989 SLAC Topical Conference,  
Stanford, CA, July 19-21, 1989, and to be  
published in the Proceedings

### Measurements of the Z Boson Resonance Parameters at SLC

C. Hearty

July 1989



1 LOAN COPY 1  
1 Circulates 1  
1 for 2 weeks 1

Bldg. 50 Library.

LBL-28547

Copy 2

## **DISCLAIMER**

This document was prepared as an account of work sponsored by the United States Government. While this document is believed to contain correct information, neither the United States Government nor any agency thereof, nor the Regents of the University of California, nor any of their employees, makes any warranty, express or implied, or assumes any legal responsibility for the accuracy, completeness, or usefulness of any information, apparatus, product, or process disclosed, or represents that its use would not infringe privately owned rights. Reference herein to any specific commercial product, process, or service by its trade name, trademark, manufacturer, or otherwise, does not necessarily constitute or imply its endorsement, recommendation, or favoring by the United States Government or any agency thereof, or the Regents of the University of California. The views and opinions of authors expressed herein do not necessarily state or reflect those of the United States Government or any agency thereof or the Regents of the University of California.

# Measurements of the $Z$ Boson Resonance Parameters at SLC\*

Christopher Hearty

Lawrence Berkeley Laboratory  
University of California  
Berkeley, California 94304

For the Mark II Collaboration

Presented at the 1989 SLAC Topical Conference  
Stanford, California, July 19–21, 1989

## 1. Introduction

This paper presents the measurement by the Mark II experiment at the SLAC Linear Collider of the parameters of the  $Z$  boson resonance. The results are updated from those presented at the SLAC Summer Institute to include all data presented in the most recent Mark II publication,<sup>1</sup> consisting of  $19 \text{ nb}^{-1}$  of data at ten different center-of-mass energies between 89.2 and 93.0 GeV.

The resonance parameters are extracted by measuring the  $Z$  production cross section at a series of center-of-mass energies (scan points) near the  $Z$  peak, then fitting these data with the theoretical cross section. The four major aspects of the analysis are the determination at each scan point of (1) the center-of-mass energy ( $E$ ), (2) the integrated luminosity, (3) the number of  $Z$  decays and (4) the expected cross section as a function of the resonance parameters, such as mass and width. I will discuss each of these steps in turn, after a brief description of the Mark II detector, then conclude with the results of the analysis.

---

\* This work was supported in part by the Director, Office of Energy Research, Office of High Energy and Nuclear Physics, Division of High Energy Physics of the U. S. Department of Energy under Contract Numbers DE-AC03-76SF00098 and DE-AC0376SF00515.

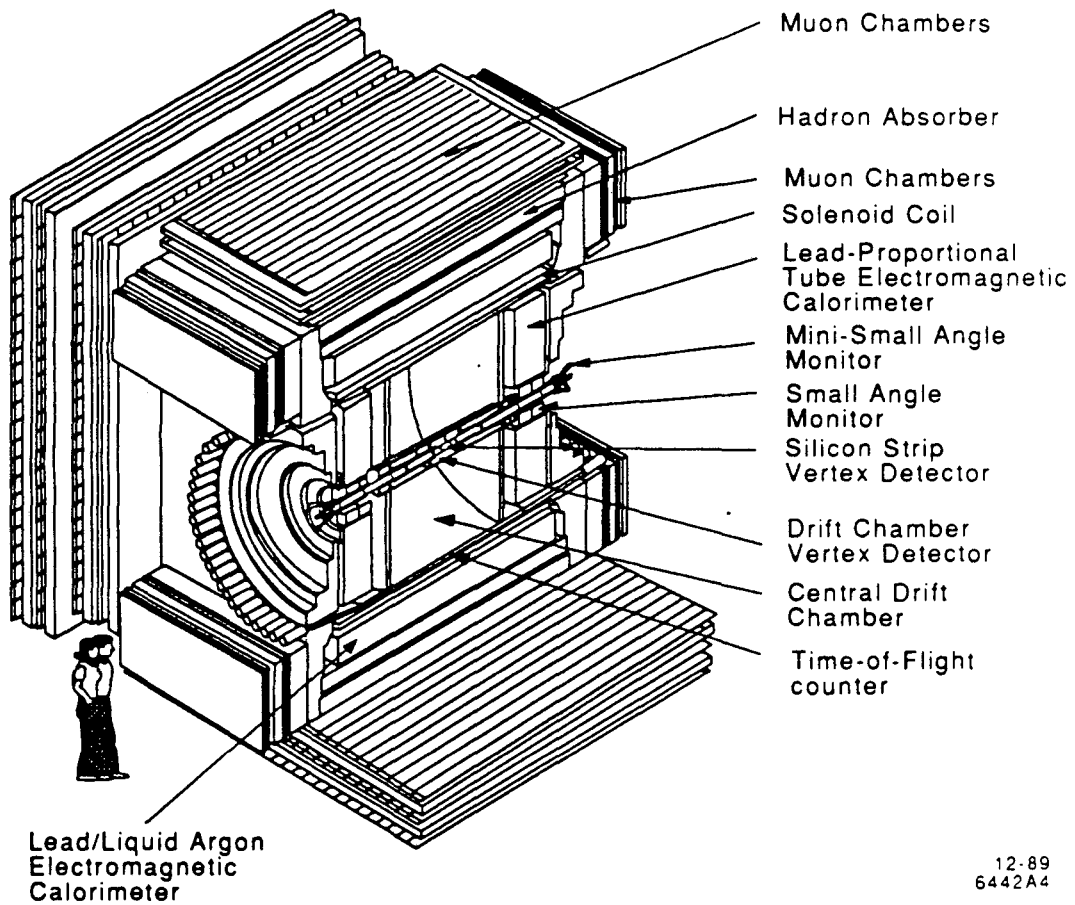
## 2. The Mark II Detector

The Mark II detector (Fig. 1) is described in detail in Ref. 2. The main components used to detect  $Z$  decays are the drift chamber and the electromagnetic calorimeters. The drift chamber, which has 72 layers and is located in a 4.75 kgauss axial magnetic field, tracks charged particles with  $|\cos \theta| < 0.92$ , where  $\theta$  is the angle with respect to the beam line. The electromagnetic calorimeters cover the region  $|\cos \theta| < 0.96$ . The calorimeters in the central region ( $|\cos \theta| < 0.68$ ) consist of alternating layers of liquid argon and lead, while the endcap calorimeters are layers of lead interspaced with proportional tube counters.

There are two detectors for the small-angle Bhabha events ( $e^+e^- \rightarrow e^+e^-$ ) used to measure the integrated luminosity (Fig. 2). The small-angle monitors (SAMs) cover the angular region  $50 < \theta < 160$  mr, where the acceptance at the inner (50 mr) edge is defined by a tungsten mask. Each SAM is 14.3 radiation lengths thick and consists of a tracking section with nine layers of drift tubes and a sampling calorimeter with six layer each of lead and proportional tubes (Fig. 3). The tracking sections have been used to determine the positional resolution of the calorimeter sections, but are not used to select events. The calorimeter sections are used to measure both the energy and position of the electron. The mini-small-angle monitors (MiniSAMs) detect Bhabha events in the angular region  $15.2 < \theta < 25.0$  mr at one end of the detector and  $16.2 < \theta < 24.5$  mr at the other. These angular regions, which are defined by tungsten masks, are asymmetric so as to substantially reduce the sensitivity of the Bhabha cross section to small movements in the interaction point (IP). Each MiniSAM is a 15 radiation length thick tungsten-scintillator sandwich divided into four azimuthal quadrants.

There are two major triggers for  $Z$  decays. The charged particle trigger requires two or more drift chamber tracks with transverse momentum greater than 150 MeV/c at  $|\cos \theta| < 0.75$ . The calorimeter trigger requires a single shower of at least 3.3 GeV in the barrel calorimeter or 2.2 GeV in the endcap calorimeter. The efficiencies for hadronic events are 97% and 95%, respectively, for these two

# MARK II AT SLC



12-89  
6442A4

Figure 1. The Mark II detector.

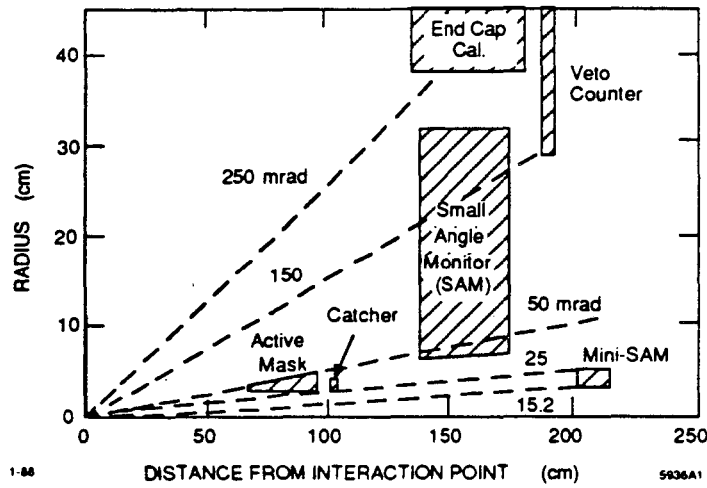


Figure 2. Locations of the SAM and MiniSAM. The relative luminosity is determined using the MiniSAM, while the absolute luminosity is found with the SAM.

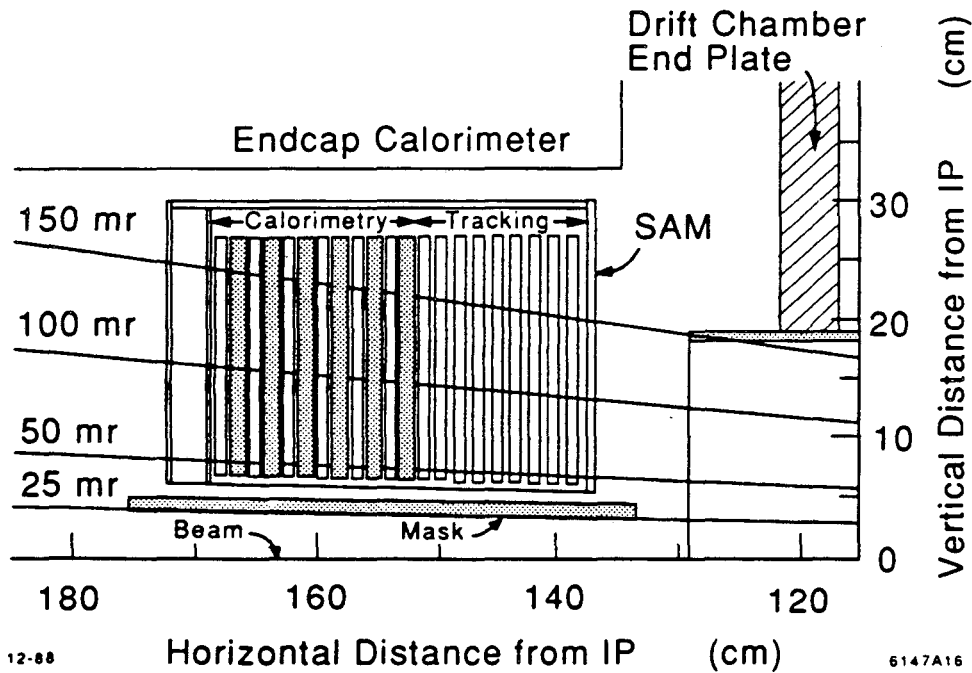


Figure 3. The small angle monitor. Bhabha events in the angular region  $50 < \theta < 160$  mr are used in the integrated luminosity measurement.

triggers; together, the efficiency is 99.8%. Addition triggers record random beam crossings and cosmic rays for diagnostic purposes and low-angle Bhabha events for the luminosity measurement. At least 6 GeV of energy in each SAM or 20 GeV in each MiniSAM is required to trigger the data acquisition system.

### 3. Measurement of the Center-of-Mass Energy

The absolute center-of-mass energy ( $E$ ) is measured on every pulse using an energy spectrometer in the extraction line of each beam.<sup>3</sup> The conceptual design of the extraction line is shown in Fig. 4. Dipole magnets before and after a precision spectrometer magnet bend the beam perpendicular to its direction, causing it to emit two swaths of synchrotron radiation. Phosphorescent screen monitors (Fig. 5) measure the distance between these swaths (approximately 27 cm) and hence the angle through which the beam was bent in the spectrometer magnet. This angle, which is proportional to  $\int Bdl/E_{\text{beam}}$ , is used with the known magnet strength to extract the beam energy  $E_{\text{beam}}$  with an uncertainty of 20 MeV. The contributions to the uncertainty are listed in Table I. There is an additional contribution to the uncertainty in  $E$  (but not in  $E_{\text{beam}}$ ) due to momentum dispersion at the IP, giving a total uncertainty in  $E$  of 35 MeV. The center-of-mass energy spread, which is typically 250 MeV, is derived from the thickness of the synchrotron stripe to an uncertainty of approximately 30% of its value.

Table I. Systematic errors in the beam energy measurement.

Source of Error	Size of Error
Mapping of the spectrometer field	5 MeV
Rotational errors in dipole alignment	16 MeV
Determination of stripe position	10 MeV
Survey errors	5 MeV
Total Uncertainty	20 MeV



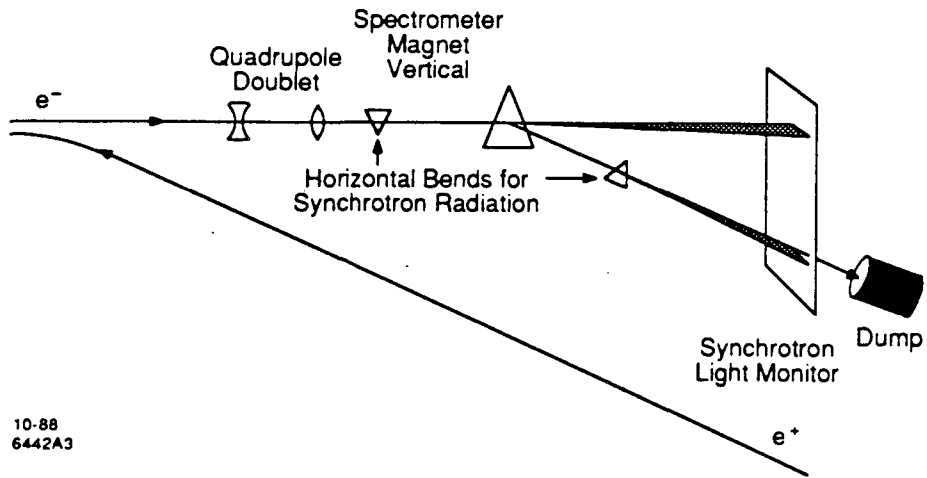


Figure 4. One of the two extraction line spectrometers used to measure the absolute beam energy.

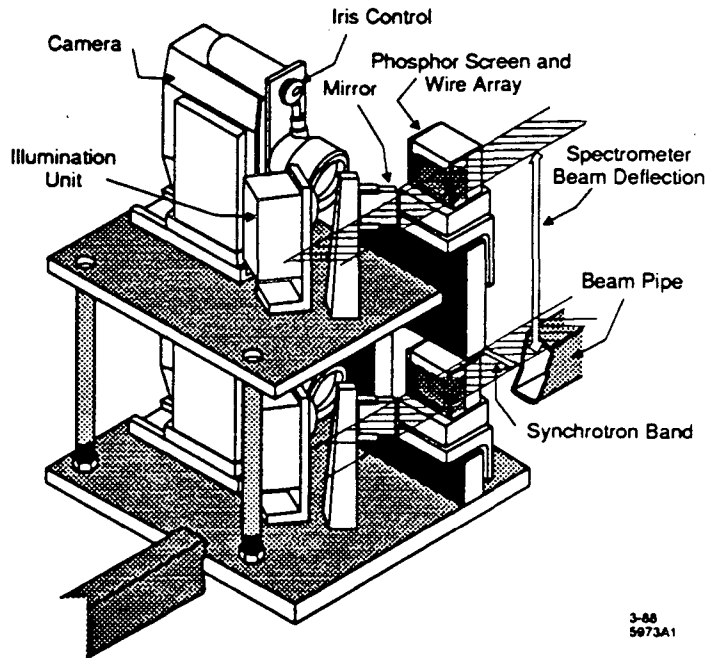


Figure 5. Phosphorescent screen monitor.

## 4. Integrated Luminosity Measurement

A typical Bhabha event in the SAM is shown in Fig. 6. Bhabha events are selected by requiring 40% of the beam energy in each SAM. There is essentially no background to these events. The position of the defining mask at 50 mr is not known accurately enough to permit the cross section for these “inclusive” events to be precisely calculated. Instead, the cross section is derived by scaling to a subset of events that fall into a fiducial volume that does have an accurately calculable acceptance. These “precise” Bhabha events are those in which  $65 < \theta < 160$  mr for both  $e^+$  and  $e^-$  showers, plus, with a weight of 0.5, events in which one shower has  $65 < \theta < 160$  mr and the other has  $60 < \theta < 65$  mr. The weighting reduces the effects of misalignments and detector resolution. The theoretically expected cross section<sup>4</sup> for events to be observed in the “precise” angular region is  $25.2 \cdot (91.1/E(\text{GeV}))^2$  nb. This includes a  $-1.9\%$  correction from the nominal cross section for this region due to reconstruction inefficiency and a  $+1.6\%$  correction due to detector resolution. (Events at  $\theta < 60$  mr can be reconstructed as  $\theta > 60$  mr.) We estimate a 2% systematic error from these detector effects and a 2% error from higher order radiative corrections, for a total systematic error of 2.8%. Multiplying this cross section by 815/484 — the ratio of “precise” to “inclusive” Bhabhas in the entire data sample — gives a cross section for events to be observed as “inclusive” Bhabhas of  $\sigma_S = 42.6 \cdot (91.1/E(\text{GeV}))^2$  nb, with a 2.9% statistical error due to the scaling error. A realignment of the 50 mr mask after the first seven scan points decreased  $\sigma_S$  by  $1 \pm 2\%$ . This factor is included in all of the following calculations.

Bhabha events in the MiniSAM are selected by requiring that a pair of quadrants of each side of the IP contain at least 25 GeV more deposited energy than the other pair of quadrants on that side. The pairs with significant energy must be diagonally opposite. In addition, all quadrants with greater than 18 GeV deposited energy must have timing information consistent with particles coming from the IP rather than striking the back of the detector 14 ns earlier. The efficiency ( $\epsilon_M$ ) depends on background conditions that can vary from scan point to scan point.

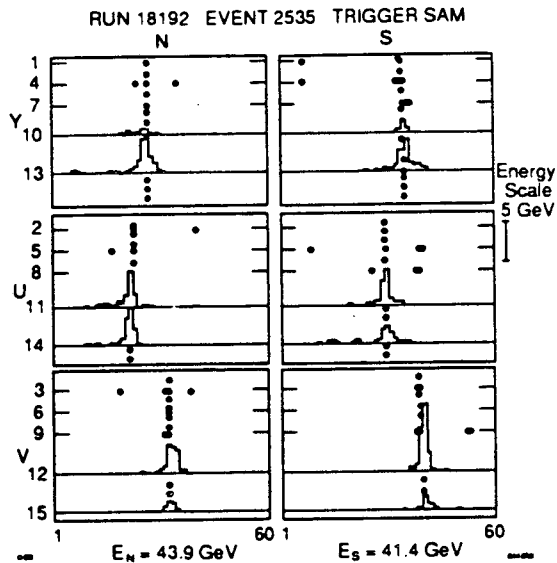


Figure 6. A Bhabha event in the small angle monitor.

It is measured for each scan point by combining random beam crossings at that energy with Monte Carlo Bhabha events and ranges from 91% to > 99%. Events in which the high energy pairs are not diagonally opposite are used to estimate the number of beam-related background events to be subtracted. The subtraction, which is 0.4% overall, ranges from 0% to 3.5% of the data at each scan point and is always less than the statistical error. The uncertainty in the number subtracted is taken to be the larger of 1% of the events at that scan point or the number itself. We cannot directly calculate the expected cross section for MiniSAM Bhabhas due to sensitivity to higher order radiative corrections and slight misalignments of the defining masks. Instead, we find it by scaling the number of events after background subtraction and efficiency correction to the number of “inclusive” SAM events. For the first seven scan points,  $\sigma_M = 227 \cdot (91.1/E(\text{GeV}))^2$  nb, while for subsequent data,  $\sigma_M = 234 \cdot (91.1/E(\text{GeV}))^2$  nb. In both cases, the statistical error due to the scaling factor is 4.5%. Because  $\sigma_M$  is substantially larger than  $\sigma_S$ , the MiniSAM dominates the measurement of relative luminosity between scan

points, while the SAM determines the absolute luminosity.

## 5. Selection of $Z$ Decay Events

We select hadronic decays of the  $Z$  and a subset of the leptonic decays based on charged tracks reconstructed by the drift chamber and showers found by the calorimeters. Charged tracks are required to emerge with transverse momentum greater than 110 Mev/c from within 1 cm of the beamline and 3 cm of the interaction point. The calorimeter showers are required to have at least 1 GeV in energy. The efficiencies of the selection criteria outlined below are measured by Monte Carlo (MC) simulation. Beam-related backgrounds are included in the detector simulation by combining data from random beam crossings with the MC data. They are found to have little effect on this analysis.

An example of a hadronic event is given in Fig. 7. Candidates for hadronic decays are required to have at least three charged tracks and at least  $0.05E$  of energy visible in each of the forward and backward hemispheres. The cut on visible energy is designed to suppress beam gas and two-photon exchange interactions, which tend to deposit energy in only one hemisphere. A MC simulation indicates that we expect 0.02 events in our data from two-photon exchange interactions. The number of beam-gas interactions that satisfy these cuts is expected to be  $< 0.2$  at the 90% confidence level (CL), since no events are found emerging from the beamline with  $3 < |z| < 50$  cm. The efficiency for  $Z$  hadronic decays to satisfy these selection requirements (including trigger), is  $\epsilon_h = 0.953 \pm 0.006$ . Differences between QCD MC models account for the largest component of the uncertainty.

We also include in our fiducial sample  $\mu$  and  $\tau$  pairs with  $|\cos \theta_T| < 0.65$ , where  $\theta_T$  is the thrust angle. We use this angular region to ensure high trigger and identification efficiency. Electron pairs are not included because of the interference from t-channel Bhabha events. Events are required to have at least  $0.1E$  of visible energy, giving an efficiency of  $99 \pm 1\%$  for muon events and  $96 \pm 1\%$  for tau events.

Run 17914 Event 656 E=92.11 GeV 18 Prong Hadronic Event  
 Triggers Charged Neutral (SST only) Mark II at SLC May 1, 1989 6:30

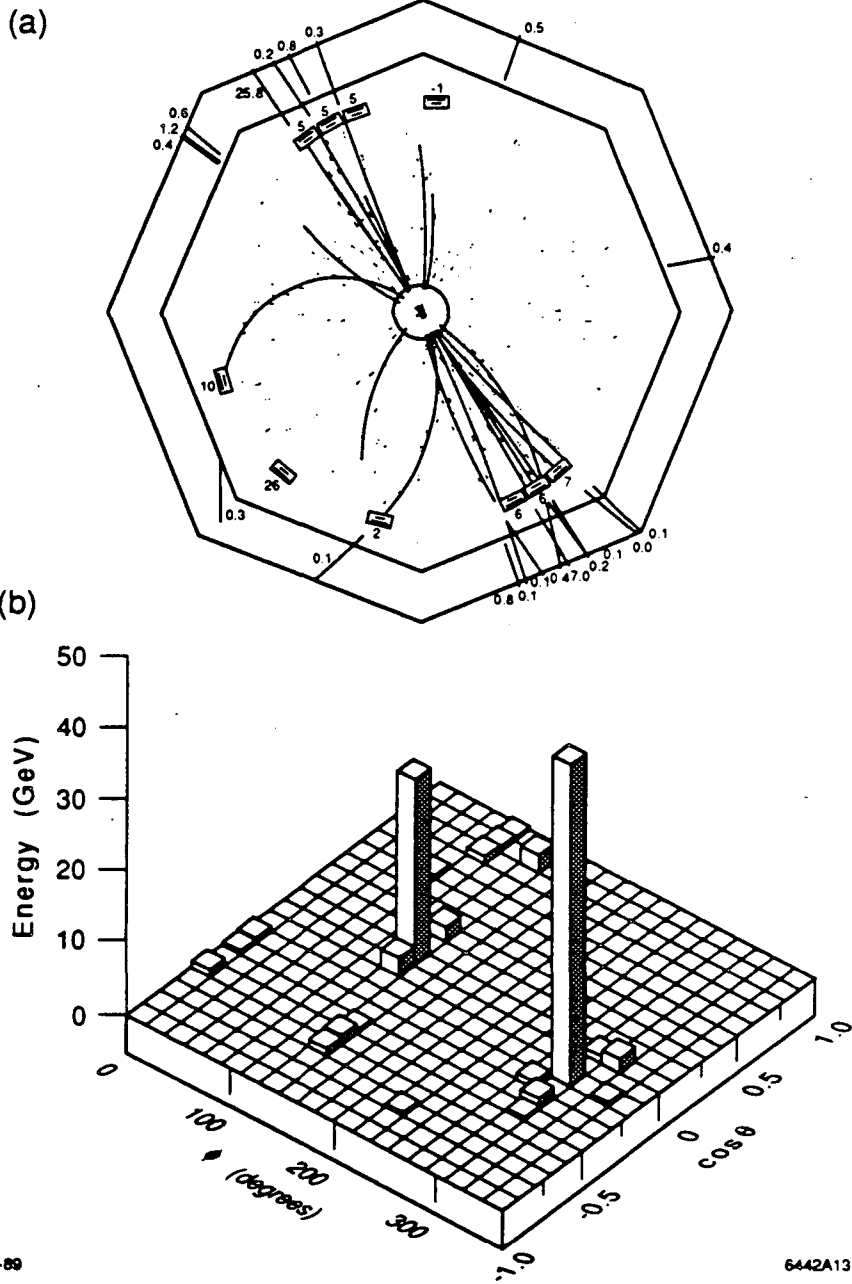


Figure 7. (a) A typical hadronic  $Z$  decay viewed along the beamline. (b) Detected energy of the event plotted as a function of  $\phi$  and  $\cos \theta$ .

Tau events with  $|\cos\theta_T| > 0.65$  that satisfy the hadronic selection criteria are rejected by a handscan.

Table II gives for each scan point the mean energy of the Bhabha events as measured by the energy spectrometer, the number of SAM “inclusive” ( $n_S$ ) and MiniSAM ( $n_M$ ) Bhabha events,  $\epsilon_M$ , the integrated luminosity, the number of hadronic and leptonic  $Z$  decays passing the selection criteria, and  $\sigma_Z^m$ . The measured cross sections  $\sigma_Z^m$  are for the production of hadronic events and muon and tau pairs with  $|\cos\theta_T| < 0.65$ . The average  $\sigma_E$  generated by the energy spread of the beams and by the pulse-to-pulse jitter and drifts of the beam energies varies from 0.22 to 0.29 GeV. The cross sections contain corrections for this energy spread that vary from +3% near the peak to -3% in the tails. That is,  $\sigma_Z^m$  represents the cross section corresponding to a center of mass energy  $\langle E \rangle$  with  $\sigma_E = 0$ . Pairs of scan points that are very close in energy — such as points one and nine — have not been combined because the two points have different cross sections for SAM and MiniSAM Bhabha events.

## 6. Fitting the Data to Extract Resonance Parameters

We estimate  $Z$  resonance parameters by constructing a likelihood function from the probability of observing, at each energy,  $n_Z$   $Z$  decays and  $n_L$  SAM and MiniSAM Bhabhas given that we have observed a total of  $n_Z + n_L$  events. We obtain for the likelihood  $L$

$$L = \prod \frac{(\epsilon\sigma_Z)^{n_Z}}{(\epsilon\sigma_Z + \sigma_L)^{n_Z+n_L}} \quad , \quad (6.1)$$

where the product is over energy scan points. The overall efficiency is  $\epsilon = 0.954$ , and  $\sigma_Z(E)$  is the calculated production cross section for hadronic events and leptonic events with  $|\cos\theta_T| < 0.65$ . The likelihood function depends on the fit parameters, such as mass and width, through the dependence of  $\sigma_Z$  on these parameters. Terms that are constant with respect to  $\sigma_Z$  have been dropped from equation (6.1).

Table II. Average energy, integrated luminosity, number of events, MiniSAM efficiency and  $\sigma_Z$  for each energy scan point. The luminosity for each scan point is given by  $\text{Lum} = (N_S + N_M)/\sigma_L$ , where  $\sigma_L = \sigma_S + \epsilon_M \sigma_M$ . The given error is the statistical error on  $N_S$  and  $N_M$  only; there are additional statistical errors on  $\sigma_L$  due to the scaling errors on  $\sigma_S$  and  $\sigma_M$  (see text). The total luminosity is calculated from the 485 “precise” SAM Bhabha events and has an overall 2.8% systematic error.

Scan Point	$\langle E \rangle$ (GeV)	$N_S$	$N_M$	$\epsilon_M$	Lum. (nb <sup>-1</sup> )	Z Decays			$\sigma_Z$ (nb)
						Had.	Lep.	Tot.	
3	89.24	24	166	0.99	0.68±0.05	3	0	3	4.5 <sup>+4.5</sup> <sub>-2.5</sub>
5	89.98	36	174	0.99	0.76±0.05	8	2	10	13.5 <sup>+6.0</sup> <sub>-4.3</sub>
10	90.35	116	617	1.00	2.61±0.10	60	2	62	24.8 <sup>+3.8</sup> <sub>-3.3</sub>
2	90.74	54	266	0.96	1.21±0.07	33	3	36	31.7 <sup>+6.8</sup> <sub>-5.5</sub>
7	91.06	170	923	0.99	4.08±0.12	114	6	120	31.6 <sup>+3.4</sup> <sub>-3.1</sub>
8	91.43	164	879	0.91	4.12±0.13	108	6	114	29.8 <sup>+3.3</sup> <sub>-2.9</sub>
4	91.50	53	275	0.99	1.23±0.07	33	6	39	34.3 <sup>+7.0</sup> <sub>-5.7</sub>
1	92.16	31	105	0.97	0.54±0.05	11	0	11	21.5 <sup>+9.2</sup> <sub>-6.6</sub>
9	92.22	128	680	0.98	3.05±0.11	67	4	71	24.3 <sup>+3.4</sup> <sub>-3.0</sub>
6	92.96	39	214	0.98	1.00±0.07	13	1	14	14.6 <sup>+5.4</sup> <sub>-4.0</sub>
Totals		815	4299		19.3±0.9	450	30	480	

A relativistic Breit-Wigner resonance shape is used to represent  $\sigma_Z$ :

$$\sigma_Z(E) = \frac{12\pi}{m_Z^2} \frac{s\Gamma_e\Gamma_f}{(s - m_Z^2)^2 + s^2\Gamma^2/m_Z^2} (1 + \delta(E)), \quad (6.2)$$

where  $s \equiv E^2$ ,  $\delta$  is the substantial correction ( $\sim -0.27$  at the pole) due to initial state radiation calculated using an analytic form,<sup>5</sup>  $\Gamma_e$  is the  $Z$  partial width for electron pairs, and  $\Gamma_f$  is the partial width for decays in our fiducial volume. The

partial widths for hadrons, muons and taus are related to  $\Gamma_f$  by  $\Gamma_f = \Gamma_h + f(\Gamma_\mu + \Gamma_\tau)$ , where  $f = 0.556$  is the fraction of all muon and tau decays that have  $|\cos \theta_T| < 0.65$ . We take the total  $Z$  width to be  $\Gamma = \Gamma_h + \Gamma_e + \Gamma_\mu + \Gamma_\tau + N_\nu \Gamma_\nu$ , where  $N_\nu$  is the number of species of neutrinos.

We have performed three fits to the data, which differ in their reliance on the minimal Standard Model. The first leaves only  $m_Z$  as a free parameter. The widths are those expected for  $Z$  couplings to the known fermions (5 quarks and 3 lepton doublets), including a QCD correction to the hadronic width.<sup>6</sup> The second fit leaves both  $m_Z$  and  $N_\nu$  as free parameters but fixes  $\Gamma_\nu$  and all other partial widths to their expected values. With this parameterization,  $N_\nu$  is derived largely from the height of the resonance. Finally, the third fit does not assume any Standard Model partial widths. Instead, we write

$$\sigma_Z(E) = \sigma_0 \frac{s\Gamma^2}{(s - m_Z^2)^2 + s^2\Gamma^2/m_Z^2} (1 + \delta(E)), \quad (6.3)$$

and fit for  $m_Z$ ,  $\Gamma$  and  $\sigma_0$  (peak production cross section, in the absence of radiative corrections, for all hadronic events and for muon and tau pairs with  $|\cos \theta_T| < 0.65$ ) as the three fit parameters. The extracted values of  $N_\nu$  or  $\sigma_0$  depend on the value of  $\epsilon$  and the absolute luminosity normalization scale, while  $m_Z$  and  $\Gamma$  are not sensitive to these quantities.

## 7. Results of the Fits

The results of these fits are displayed in Fig. 8 and Table III. We conclude that  $m_Z = 91.14 \pm 0.12 \text{ GeV}/c^2$ . The uncertainty includes systematic errors added in quadrature, the largest of which is the 35 MeV due to the absolute energy measurement. The systematic error in  $m_Z$  due to uncertainty in the initial state radiation correction is estimated to be less than  $10 \text{ MeV}/c^2$ .<sup>5</sup>

The second fit gives  $N_\nu = 2.8 \pm 0.6$ , which is equivalent to a partial width to invisible decay modes of  $N_\nu \Gamma_\nu = 0.46 \pm 0.10 \text{ GeV}$ . The luminosity uncertainty



contributes 0.45 to the error in  $N_\nu$ . The 95% CL limit is  $N_\nu < 3.9$ , which excludes to this level the presence of a fourth massless neutrino species within the Standard Model framework.

Table III.  $Z$  resonance parameters. The three fits are described in the text.

Fit	$m_Z$ GeV/ $c^2$	$N_\nu$	$\Gamma$ GeV	$\sigma_0$ nb
1	$91.14 \pm 0.12$	–	–	–
2	$91.14 \pm 0.12$	$2.8 \pm 0.6$	–	–
3	$91.14 \pm 0.12$	–	$2.42^{+0.45}_{-0.35}$	$45 \pm 4$

The third fit yields  $\Gamma = 2.42^{+0.45}_{-0.35}$  GeV, in good agreement with the Standard Model value of 2.45 GeV. The MiniSAM background subtraction error, which is the largest systematic error, contributes 50 MeV to the uncertainty. The third fit value for  $\sigma_0$  of  $45 \pm 4$  nb agrees well with the value of 43.6 nb calculated using  $m_Z = 91.14$  GeV/ $c^2$  and Standard Model partial widths. The corresponding cross section for hadron decays is  $42 \pm 4$  nb. The maximum production cross section (including radiative corrections), which occurs approximately 90 MeV above the pole due to initial state radiation, is  $33 \pm 3$  nb for all events in our fiducial region, or  $31 \pm 3$  nb for hadronic events only.

The electroweak mixing angle, defined<sup>7</sup> as  $\sin^2 \theta_W \equiv 1 - m_W^2/m_Z^2$ , is related to  $m_Z$  through

$$\sin 2\theta_W = \left( \frac{4\pi\alpha}{\sqrt{2}G_F m_Z^2 (1 - \Delta r)} \right)^{\frac{1}{2}}, \quad (7.1)$$

where  $\Delta r$  represents the effects of higher order radiative corrections. Because  $\Delta r$  is sensitive to the masses of heavy particles, the top quark mass and Higgs mass must be specified to calculate  $\sin^2 \theta_W$  from  $m_Z$ . For  $m_t = m_H = 100$  GeV/ $c^2$  and

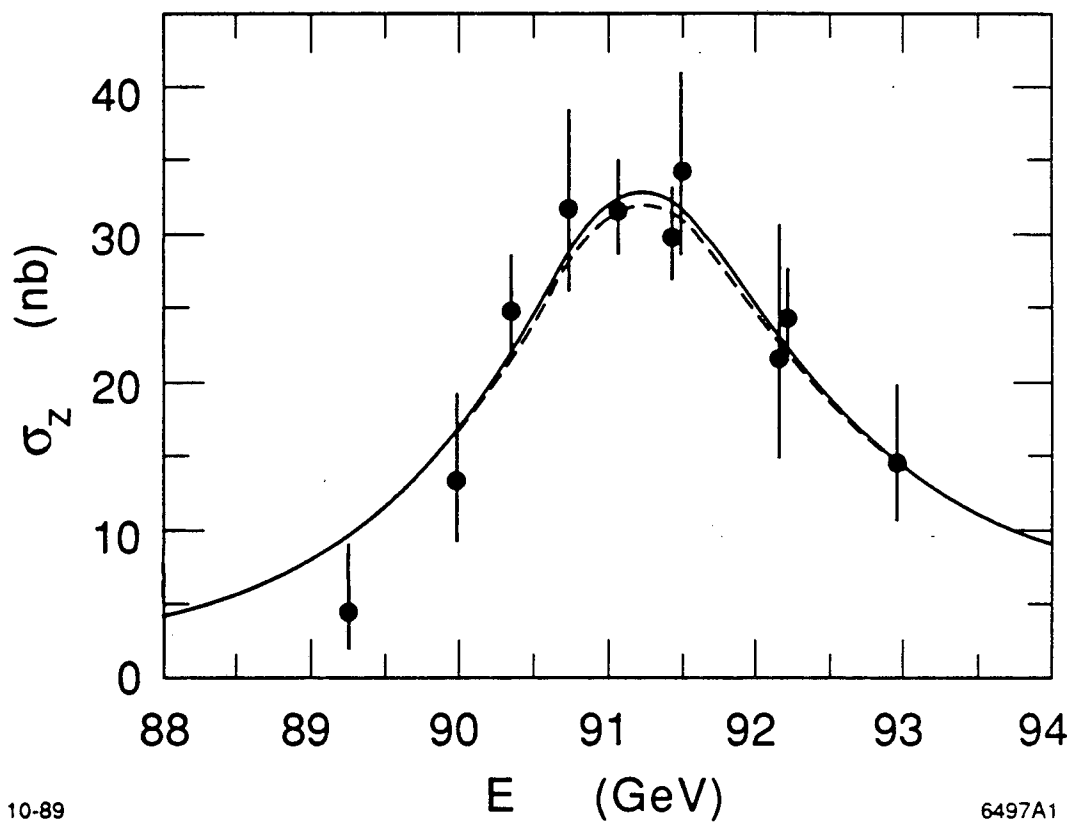


Figure 8.  $e^+e^-$  annihilation cross sections to all hadronic events plus  $\mu$  and  $\tau$  pairs with  $|\cos\theta_T| < 0.65$ . The dashed curve represents the result of the first fit, which assumes all standard model partial widths and  $N_\nu = 3$  and leaves only  $m_Z$  as a free parameter. The solid curve represents the second and third fit results, which are indistinguishable. The second fit is similar to the first, except that both  $m_Z$  and  $N_\nu$  are fit parameters, while the third fit includes no assumptions about partial widths.

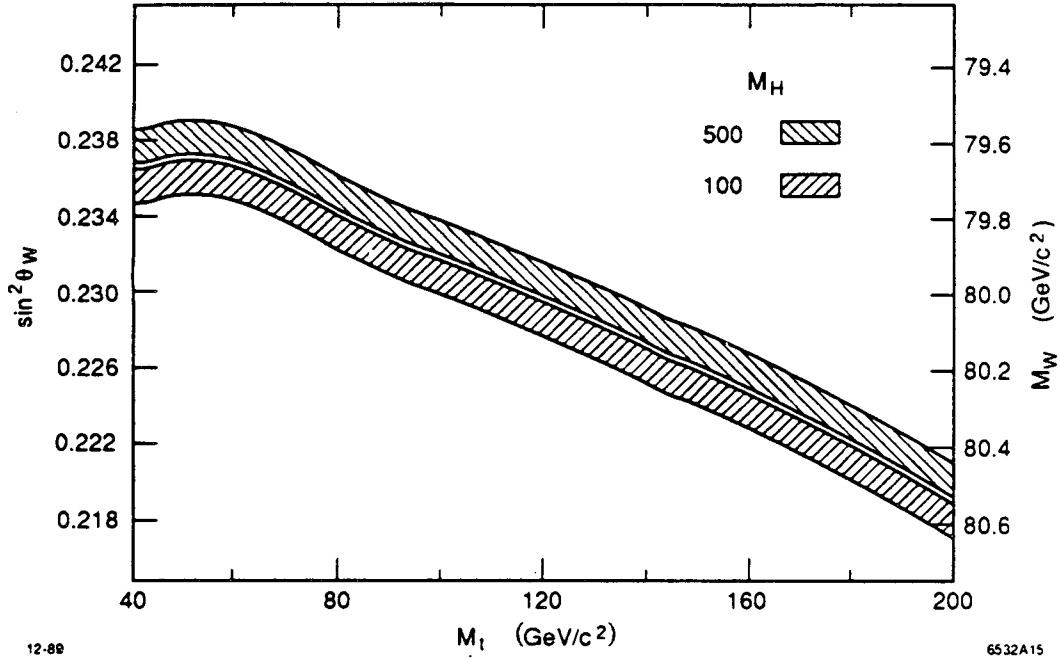


Figure 9. Value of  $\sin^2 \theta_W$  as a function of the top quark mass, for two Higgs boson masses. The widths of the bands are due to the uncertainty in the mass of the  $Z$ .

our value for the  $Z$  mass,  $m_Z = 91.14 \pm 0.12 \text{ GeV}/c^2$ , we obtain

$$\sin^2 \theta_W = 0.2304 \pm 0.0009. \quad (7.2)$$

The dependence of  $\sin^2 \theta_W$  on  $m_t$  and  $m_H$  is shown in Fig. 9.

## REFERENCES

1. G. S. Abrams *et al.*, *Phys. Rev. Lett.* **63**, 2173 (1989).
2. G. S. Abrams *et al.*, *Nucl. Instrum. Methods* **A281**, 55 (1989).
3. J. Kent *et al.*, SLAC-PUB-4922 (1989); M. Levi, J. Nash and S. Watson, *Nucl. Instrum. Methods* **A281**, 265 (1989); M. Levi *et al.*, SLAC-PUB-4921 (1989).
4. F.A. Berends, R. Kleiss, W. Hollik, *Nucl. Phys.* **B304**, 712 (1988), S. Jadach, B. F. L. Ward, *Phys. Rev. D* **40**, 3582 (1989).
5. R. N. Cahn, *Phys. Rev. D* **36**, 2666 (1987), Eqs. 4.4. and 3.1. See J. Alexander *et al.*, *Phys. Rev. D* **37**, 56 (1988) for a comparison of different radiative correction calculations.
6. Widths are calculated using the program EXPOSTAR, assuming  $m_{\text{top}} = 100 \text{ GeV}/c^2$ . D. C. Kennedy *et al.*, *Nucl. Phys.* **B321**, 83 (1989).
7. A. Sirlin, *Phys. Rev. D* **22**, 971 (1980).

LAWRENCE BERKELEY LABORATORY  
UNIVERSITY OF CALIFORNIA  
INFORMATION RESOURCES DEPARTMENT  
1 CYCLOTRON ROAD  
BERKELEY, CALIFORNIA 94720